

# Heat and momentum transfer of a buoyant blob in low Prandtl number fluids

Kazuto Igaki, Ryuta Abe, Yuji Tasaka, Ichiro Kumagai and Yuichi Murai  
 Graduate School of Engineering, Hokkaido University, N13-W8, Kita-ku, Sapporo, 060-8628, Japan  
 e-mail: igaki@ring-me.eng.hokudai.ac.jp

The motivation of this study is obtaining characteristic features of heat and momentum transfer in low  $Pr$  fluids through a detailed measurement using UVP. As a preliminary study, two types of experiments were conducted with liquid gallium. One is with respect to “thermal”, instantaneous release of a thermal blob into the ambient fluid, and the other is an experiment of a starting plume. In the former experiments, we found that thermal buoyancy affects the convective behavior of the blob, even though the characteristic time for thermal diffusivity in liquid gallium is large. It was observed that the vortex structure in the buoyant blob remains or decays, depending on the direction of the working buoyant force. In another experiment, we succeeded in observing the motion of the thermal plume in liquid gallium. From simultaneous measurement of velocity and temperature field, we visualized some features of a laminar starting plume such as translational velocity and entrainment.

**Keywords:** Heat and momentum transfer, Low Prandtl number, Liquid metal, Thin container, Ultrasonic velocity profiling

## 1 INTRODUCTION

Thermal plumes are seen in wide range of field from natural convections to industries. The convective elements driven by thermal buoyancy are generally believed to make large scale convections such as Rayleigh-Benard convection [1]. Accordingly, investigations of their generation and rising motions have significant rolls in basic study of thermal convection. Their convective motions are often described by Rayleigh number ( $Ra$ ) and Prandtl number ( $Pr$ ). There are many experiments and studies with interests in thermal convection regarding fluids at higher  $Pr$  than unity [2-3]. On the other hand, the thermal convection in low  $Pr$  fluids such as liquid metals (where  $Pr$  approximately range from 0.01 to 0.1) has not been investigated enough compared to that of higher  $Pr$  fluids. However, the heat transfer in lower  $Pr$  fluids is believed to be very different from higher  $Pr$  fluids [4-5]. The reason why the experimental studies on low  $Pr$  fluids are so few is that their convective motions cannot be visualized optically. In recent years, the advancement of measurement techniques using ultrasonic waves makes it possible to obtain a spatio-temporal velocity field even for opaque fluids.

Our group is applying the Ultrasonic Velocity Profiling (UVP) on thermal convections in low  $Pr$  fluids. In the past, we conducted UVP measurement on thermal plumes in a circular cylinder. However, we could do little meaningful discussion since velocity measurement using the UVP is a line measurement. Then, we employed a thin container which can restrain the complexity of the three dimensional flow and exploit the capabilities of the UVP. In addition, Thermo-chromic Liquid Crystals (TLCs) was pasted on an inner wall of the container

to visualize the temperature field on the basis that the temperature difference is small in the depth direction. Therefore, this thin container has enabled us to obtain the velocity and temperature as a field simultaneously.

It may be guessed that buoyancy effects in low  $Pr$  fluids decays rapidly, considering its large thermal diffusivity. Beginning with this question, we conducted two types of experiments in the thin container as a preliminary study for a thermal plume. These experiments aim to investigate how buoyancy works on the heat and momentum transfer in low  $Pr$  fluids. First, we ran experiments of “thermal”, instantaneous release of a thermally buoyant blob. We injected small quantity of fluid with temperature difference among the ambient fluid layer. Then, we observed how the vortex structure in a buoyant blob decays, where buoyancy effects were expected to emerge. Second, we conducted a brief experiment of a cold plume. The fluid layer was cooled from above. In this trial, we succeeded in measuring the behavior of a starting plume in low  $Pr$  fluid.

## 2 APPARATUS AND METHOD

### 2.1 Working fluid

Liquid gallium whose melting point is 30°C was used as a working fluid because it is easier to treat in laboratory experiments than other liquid metals such as sodium or mercury. Its kinematic viscosity and thermal diffusivity are  $3.2 \times 10^{-7} \text{m}^2/\text{s}$  and  $1.2 \times 10^{-5} \text{m}^2/\text{s}$  respectively, so that  $Pr$  of liquid gallium equals 0.025. Sound speed in liquid gallium we applied for UVP measurement is around 2860 m/s. The sound speed has different values depending on working temperature, but this effect is enough small for our experiments to disregard it.

## 2.2 Experimental set-up and method

The experiments were conducted in a thin acrylic container illustrated in Figure 1 whose size is 150mm×270mm×15mm. The container was filled with liquid gallium up to 205mm in height. A nozzle with a film of latex membrane stretched tightly on the outlet is mounted on top part of the container. As soon as the membrane is broken by a needle, the liquid gallium which has temperature difference among the fluid layer is introduced into the container by gravity force. The height of fluid level in the nozzle (which is described by  $h$ ) is 35mm. Cross-sectional dimensions of the nozzle are 20mm×8mm.

Three ultrasonic transducers (A, B and C) were installed on the container to measure velocity distributions as shown in Figure 1. Their basic frequency is 4MHz. Transducer A is for the measurement on the vertical axis to observe the advection of the injected liquid gallium blob, and the other transducers are for the horizontal axis to determine the vortex structure of the blob. Only two transducers A-B or A-C were used for simultaneous measurements to reduce interferences. The system used for signal processing was UVP, UVP monitor model Duo (Met-Flow S. A.). As ultrasonic reflection particles, fine powder of  $ZrB_2$  was suspended in the liquid gallium. This tracer particle has 50 $\mu$ m in diameter and 6.17kg/m<sup>3</sup> in density.

To visualize the temperature field, TLCs whose range of color developing temperature is from 35°C to 40°C was painted on the surface of the inner plane. The color variation of TLCs which represents the temperature near the inside wall, was recorded by a high-speed video camera placed in front of the container. The white light created by metal halide lamp illuminated the wall.

The container is set in a temperature-controlled bath to regulate the ambient temperature. The experimental conditions regarding temperature are listed on Table 1. Here,  $T_0$  means initial temperature of the fluid layer. In Exp. (a), experiments of "thermal",  $T_b$  represents initial temperature of a blob at the nozzle. The initial temperature difference between a blob and the ambient is defined as  $\Delta T (=T_0-T_b)$ . In the experiment of a starting plume (Exp. (b)),  $T_s$  means temperature of a cooling source. The nozzle with frozen water was mounted above the fluid layer, not for injection of fluids but as a cooling source.

Table 1: Experimental conditions regarding temperatures

	$T_0$ (°C)	$T_b$ (°C)	$\Delta T (=T_0-T_b)$ (°C)
Exp. (a1)	47	32	15
Exp. (a2)	32	47	-15
	$T_0$ (°C)	$T_s$ (°C)	$\Delta T (=T_0-T_s)$ (°C)
Exp. (b)	42	0.0	42

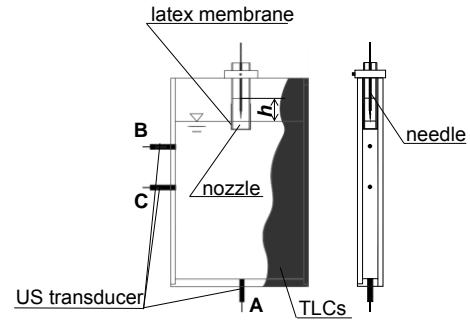


Figure 1: Schematic diagram of experimental container

## 3 RESULTS AND DISCUSSION

### 3.1 Exp. (a): Injection of a buoyant blob

Figure 2 shows the temperature field just after an injection in Exp. (a1). The gray scale color represents Hue information extracted from raw images with RGB brightness components. Hue refers to a pure color divided from other elements of color, so that it is advantage in analyzing color. More detail information of treatment with color is introduced in Dabiri, *et al.* (1991) [6]. Here, temperature rises as Hue approaches to 240 degrees. As shown in the figure, just after the injection was started, a thermally buoyant blob rolled up the shear layer and, in result, formed a pair of vortex structures. From the figure, it was confirmed that the buoyant blob had gained an initial circulation and buoyancy.

Spatio-temporal velocity field on measurement line A was obtained as shown in Figure 3(a). To compare the translational behavior among the two temperature conditions:  $\Delta T=15$  ( $T_0>T_b$ ) and  $\Delta T=-15$  ( $T_0<T_b$ ), we picked up the peak velocity locations and they were plotted in Figure 3(b). As shown in Figure 3(b), there are no remarkable differences found among the two conditions in terms of vertical velocity distribution.

On the horizontal axis, however, spatio-temporal velocity distributions of the two temperature conditions have notable disparity. Figure 4 and Figure 5 show velocity distributions on horizontal axis; Figure 4 was obtained in Exp. (a1) and Figure 5 was in Exp. (a2). In the each figure, (a) is velocity distribution on measurement line B and (b) is that on measurement line C. In Figure 4, clear velocity patterns of vortex structure could be observed. Here, vortex structure was confirmed from the characteristics of the velocity field. The feature of the velocity field is that the relation of the opposite signed peak of temporal velocity distribution reverses as time passed. In Figure 4 (a) and (b), those clear velocity patterns of vortex in both measurement line (B and C) indicate that a buoyant blob remain and expand its vortex structure. This insight is illustrated in Figure 4 (a') and (b'). On the other hand, velocity distribution with opposite temperature condition ( $T_0<T_b$ ) had similar but quite

different patterns as shown in Figure 5. In terms of measurement line C, the velocity pattern was similar to Figure 4 but latter half does not have clear peak velocity locations. The moderately sloped velocity distribution in latter half of a blob shows us that the blob has stretched structure as shown in Figure 5(b'). Those differences are due to following reasons. In these experiments, whether a blob remains vortex structure or not is attributed to the relation between the direction of buoyancy and advection. In experiment (a1), the thermally buoyant force worked downward which was the same direction to its translational direction. Contrary to that case, the buoyancy worked upward in the opposite temperature relation, in experiment (a2). Thus, buoyancy caused stretching or decaying the vortex structure. It is considered that when the direction of buoyancy corresponds to the local flow direction, the effects of buoyancy force easily emerge. Consequently, the stretching of the structure is observed in the latter half of the blob.

It was maintained, so far, that buoyancy worked on the behavior of the blob. To validate the buoyancy effects, we estimated the order of time scale for thermal diffusion using the thermal diffusivity. Here, the time scale  $\tau_d$  is defined as  $\tau_d = L^2/\kappa$ , where  $L$  is representative length, derived from the cubic root of the volume for the injected blob. The value of  $L$  is 18mm. Therefore,  $\tau_d$  equals 27s. Considering the time scale of these experiments, about 2s or 3s, the value of  $\tau_d$  indicates thermal buoyancy sufficiently has potential to influence on the behavior of the blob.

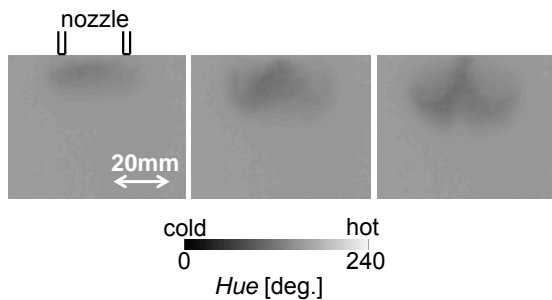


Figure 2: Formation of a pair-vortex structure

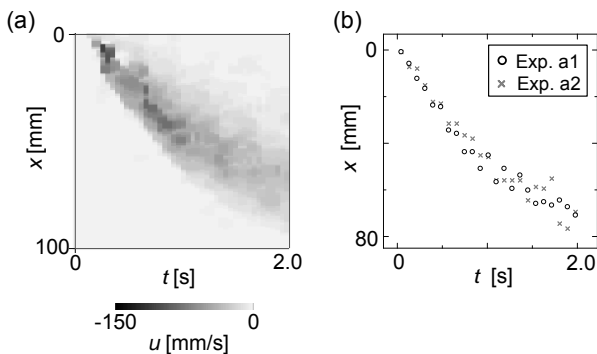


Figure 3: (a) Velocity distribution on vertical axis and (b) temporal locations of peak velocity

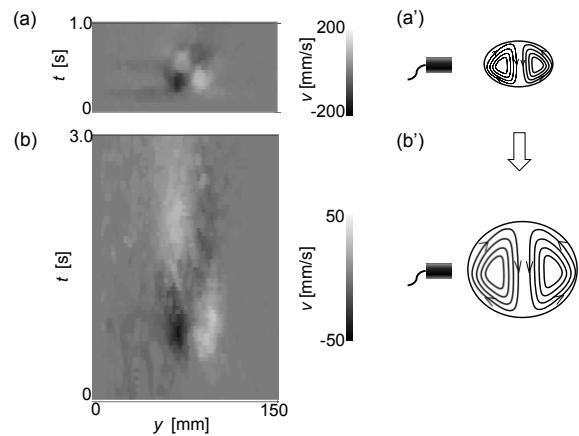


Figure 4: Velocity distributions obtained in Exp. (a1) and schematic images of the structure in the blob: (a-a') on measurement line B, (b-b') on measurement line C

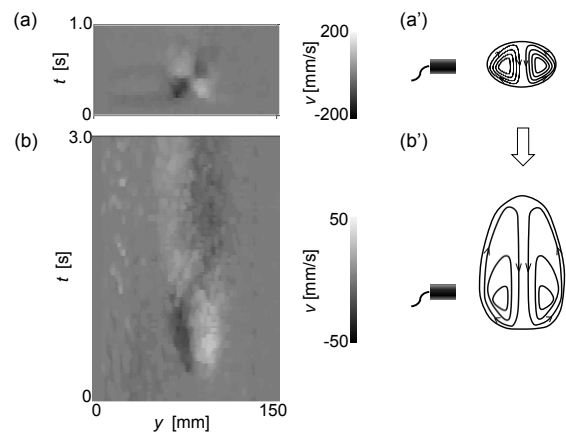


Figure 5: Velocity distributions obtained in Exp. (a2) and schematic images of the structure in the blob: (a-a') on measurement line B, (b-b') on measurement line C

### 3.1 Exp. (b): Starting plume cooled from above

The experiment of the cold plume was conducted in the same container as described previously. Figure 6(a) shows the temperature field represented by *Hue* information. In the figure, the behavior of a cold plume was observed in temperature field. Then, we detected the head of a plume and calculated its translational velocity from the images. At first, the time line image in Figure 6(b) was prepared. In Figure 6(b), the gradient of the time development image of *Hue* information means the velocity of heat transfer. The gradient was calculated in the time range from  $t=10$ s to  $t=30$ s and the value was 4.3 mm/s. This velocity is defined as  $u_h$ . On the other hand, Figure 7 shows a spatio-temporal velocity distribution on the measurement line A which is for vertical axis. The gradient of peak velocity locations is seen in the figure, which indicates the motion of plume head. Thus, the gradient means the velocity of momentum transfer. We estimated the velocity  $u_m$ , which was about 4.0 mm/s. Here, the  $u_m$  was smaller than  $u_h$ . It can be said that the speed of heat transfer is faster than that of momentum transfer.

Then, we performed order estimation of the velocity scale of thermal diffusion. Here, the velocity scale  $U_d$  is defined as  $U_d=L/\kappa$ . The value of  $L$  is 20mm, width of the cooling source. Consequently,  $U_d$  computed in 0.6mm/s. Given  $U_d$  can be calculated from  $\Delta u (=u_h-u_m)$ , the  $U_d (=0.6\text{mm/s})$  and  $\Delta u (=0.3\text{mm/s})$  have reasonable agreement. It should be considered that the starting plume descended with an angle due to experimental difficulties. Additionally, the  $u_h$  reflected only the large valued  $Hue$  information, so that the small variation of  $Hue$  was disregarded.

Figure 8(a) shows a velocity distribution on measurement line C which is for horizontal axis. The flow structure indicating entrainment at plume head was seen in the figure, though the latter half part of the plume head was not so distinct. In the figure, around  $t=10\text{s}$ , negative velocity was seen in wide range for space, compared to positive velocity. This is because the plume head entered in the measurement line not orthogonally but with an angle. In addition, the latter half or stem of the plume slid forward on  $y$  axis, horizontal axis. A schematic image in Figure 8(b) is a possible example of these interpretations of the velocity distribution. Also in temperature field, these features of the starting plume behavior, such as descending obliquely and shifting toward  $y$  direction, were observed as shown in Figure 6(a).

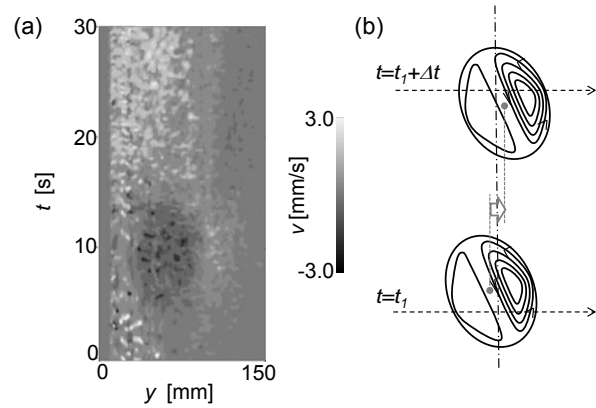


Figure 8: (a) Velocity distribution of a starting plume on measurement line C (for horizontal axis) and (b) a schematic image of swaying forward on  $y$  axis

#### 4 CONCLUSION AND REMARKS

Two types of experiments were conducted in order to investigate whether buoyancy works or not and how buoyancy affects the convective motions in low  $Pr$  fluids. From measurements of spatio-temporal velocity field and temperature field by means of UVP and TLCs, following insights were obtained.

In Exp. (a), buoyancy effects on decaying the vortex structure was confirmed. When the direction of buoyant force was opposite to that of the advection of the blob its vortex structure decayed rapidly. Furthermore, the buoyancy effects emerged not in the translational behavior but in the extension of the vortex structure.

In Exp. (b), though it is necessary to take account of several experimental matters, we have succeeded in measurement of the features of the starting plume, such as translation and entrainment. From the perspective of flow visualization for thermal plumes in low  $Pr$  fluids, these experimental results are meaningful examples in the study of the thermal convection. Accordingly, detailed experimental study of thermal plumes in low  $Pr$  fluids is our next step.

#### REFERENCES

- [1] J. Zhang, *et al.*: Non-Boussinesq effect: Thermal convection with broken symmetry, *Phys. Fluids*, 9 (1997), 1034-1042.
- [2] G. Zocchi, *et al.*: Coherent structures in turbulent convection, and experimental study, *Physica A*, 166 (1990), 387-407.
- [3] T. S. Pottebaum, *et al.*: The pinch-off process in a starting buoyant plume, *Exp. Fluids*, 37 (2004), 87-94.
- [4] R. Verzicco, *et al.*: Prandtl number effects in convective turbulence, *J. Fluid Mech.*, 383 (1999), 55-73.
- [5] C. A. H. Majumder, *et al.*: Four dynamical regimes for a starting plume model, *Phys. Fluids*, 16 (2004), 1516-1531.
- [6] D. Dabiri, *et al.*: Digital particle image thermometry: The method and implementation, *Exp. Fluids*, 11 (1991), 77-86.

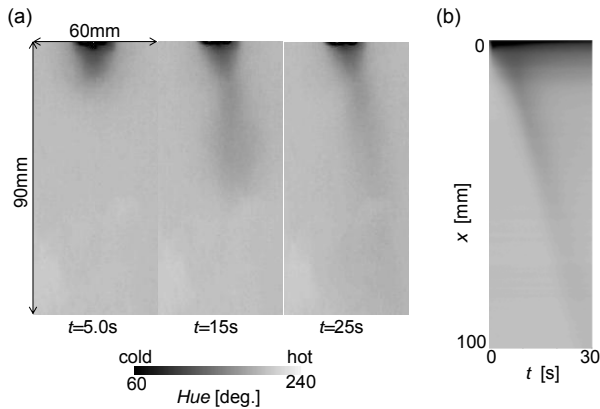


Figure 6: Plume motions observed in  $Hue$  information

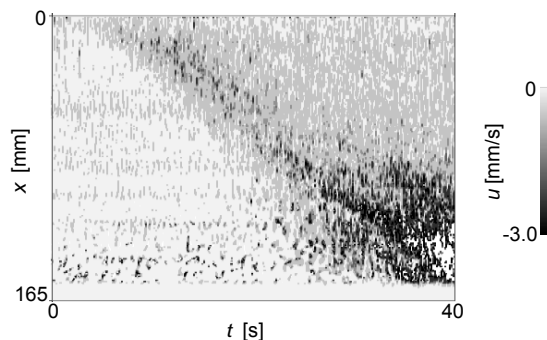


Figure 7: Velocity distribution of a starting plume on measurement line A (for vertical axis)